

Preparation and Properties of Redox-Responsive Micelles Based on Carboxymethyl Hydroxypropyl Chitosan

Jianrui Liu^a and Yongqin Zhang^{*}

Qingdao University of Science and Technology, Qingdao 266061, China

Abstract. By employing carboxymethyl hydroxypropyl chitosan (HPCMS) as the hydrophilic unit, deoxycholic acid (DOCA) as the hydrophobic unit, and cystamine (CYS) as the linker, the synthesis involved a two-step amidation process. Initially, DOCA's carboxyl group reacted with one amino end of CYS, resulting in deoxycholic acid-cystamine (DOCA-SS-NH₂). Subsequently, amidation was carried out between HPCMS's carboxyl group and the amino group of DOCA-SS-NH₂, yielding the amphiphilic polymer carboxymethyl hydroxypropyl chitosan-cystamine-deoxycholic acid (HPCMS-SS-DOCA). Leveraging the self-assembly characteristics of this amphiphilic polymer, blank micelles demonstrating redox responsiveness and drug-loaded micelles encapsulating doxorubicin (DOX) were formulated through dialysis. Fourier-transform infrared spectroscopy (FTIR) and proton nuclear magnetic resonance (¹H NMR) were deployed to determine the chemical structures of HPCMS, DOCA-SS-NH₂, and the resulting polymer HPCMS-SS-DOCA. Dynamic light scattering (DLS) and transmission electron microscopy (TEM) were utilized to examine the particle size distribution and morphology of the polymer micelles. The ultraviolet spectrophotometer assessed the drug loading and encapsulation efficiency of the drug-loaded micelles, while in vitro drug release assays investigated the redox-responsive drug release performance of the drug-loaded micelles. FTIR and ¹H NMR results confirmed the successful synthesis of the amphiphilic polymer HPCMS-SS-DOCA. DLS and TEM results demonstrated that both blank and drug-loaded micelles are spherical, with small particle sizes and uniform distribution. The drug-loaded micelles exhibited an average particle size of 262.9 nm and a polydispersity index (PDI) of 0.189. The drug loading and encapsulation efficiencies were found to be 13.23% and 66.14%, respectively. In a reductive environment, in vitro drug release assays indicated that the drug release amount within 48 hours was 52.67%, while in the non-reductive environment, the drug release amount within 48 hours is only 25.57%, indicating that this polymer micelle has good redox responsiveness.

1 Introduction

Cancer has emerged as a critical health threat for humans, boasting a high frequency and fatality rate^[1]. Chemotherapy stands out as a prevalent approach to combat cancer. Nevertheless, most chemotherapy agents are hydrophobic and exhibit poor water solubility, leading to nonspecific delivery and severe adverse effects. Polymer micelles offer a promising solution to enhance the solubility of hydrophobic drugs and improve targeting. These micelles are structured with a hydrophobic core internal and a hydrophilic shell external^[2]. The hydrophobic core serves to encase hydrophobic drugs, while the hydrophilic shell functions to shield the encapsulated drugs from the surroundings. Despite the enhanced permeability and retention (EPR) effect of tumors^[3], facilitating the accumulation of drug-loaded micelles around tumor cells, efficient drug release solely relying on the EPR effect remains challenging. Therefore, incorporating stimulus-responsive functional groups into micelle polymers can address these issues. A myriad of stimulus-responsive micelles^[4, 5] have been developed, particularly redox-type polymer micelles featuring

disulfide bonds in their structure. Disulfide bonds exhibit no physiological harm and maintain stability within normal human bodies. However, these bonds can be cleaved by the increased levels of reduced glutathione (GSH) in tumor cells, approximately four times higher than in normal tissues^[6], through thiol-disulfide exchange^[7]. Consequently, the controlled release of drugs from polymer micelles within tumor tissues can be achieved, fostering targeted delivery.

Chitosan, as the only polycationic polysaccharide among the polysaccharides discovered in nature^[8], has many excellent properties due to its unique amino structure, including biodegradability^[9], biocompatibility^[10], antibacterial^[11], and other physiological characteristics, so it has been widely used in many fields. However, the water solubility of chitosan is poor and it can only dissolve in the acidic pH range such as acetic acid and lactic acid^[12], which greatly limits the application of chitosan. Usually, hydroxypropyl and carboxymethyl modifications are carried out on chitosan to improve its water solubility.

In this paper, carboxymethyl hydroxypropyl chitosan (HPCMS) is used as the hydrophilic group, and the

^{*} Corresponding author: zyq0205@qust.edu.cn; ljr6660130@163.com

hydrophobically modified deoxycholic acid (DOCA-SS-NH₂) modified by cystamine is connected through amidation reaction to synthesize a redox-responsive amphiphilic polymer (HPCMS-SS-DOCA). By utilizing dialysis, the polymer will spontaneously form micelles in a water-based solution. The drug-loading and in vitro drug-release behaviors of the micelles loaded with the anti-cancer medication doxorubicin (DOX) will be assessed as a representative drug model.

2 Experimental section

2.1 Materials

Carboxymethyl hydroxypropyl chitosan (HPCMS, with a degree of deacetylation of 47.3%, a degree of hydroxypropyl substitution of 0.3, and a degree of carboxymethyl substitution of 1.011), self-made in the laboratory; formamide, concentrated hydrochloric acid (36%~38%), phosphotungstic acid, triethylamine, isopropanol, dimethyl sulfoxide (DMSO), disodium hydrogen phosphate dodecahydrate, sodium dihydrogen phosphate dihydrate, Sinopharm Chemical Reagents Co., Ltd.; N-hydroxy succinimide (NHS), deoxycholic acid (DOCA), N, N-dimethylformamide (DMF), N,N'-diisopropyl-carbodiimide (DIC), 1-ethyl-(3-dimethylaminopropyl) carbodiimide hydrochloride (EDC), potassium bromide (KBr), doxorubicin hydrochloride (DOX), Shanghai Aladdin Biochemical Technology Co., Ltd.; cystamine dihydrochloride (CYS), Sigma-Aldrich (Shanghai) Trading Co., Ltd.; glutathione (reduced form), Shanghai Macklin Biochemical Technology Co., Ltd.; heavy water (D₂O, 99.9%), deuterated hydrochloric acid (HCl, 99.5%), deuterated dimethyl sulfoxide (DMSO-d₆), Adamas Reagent Co., Ltd.; the experimental water is all ultrapure water, self-made in the laboratory.

2.2 Synthesis

The synthetic route of HPCMS-SS-DOCA is shown in Fig. 1, and the specific steps of synthesis are slightly modified according to the method reported in the literature^[1,3].

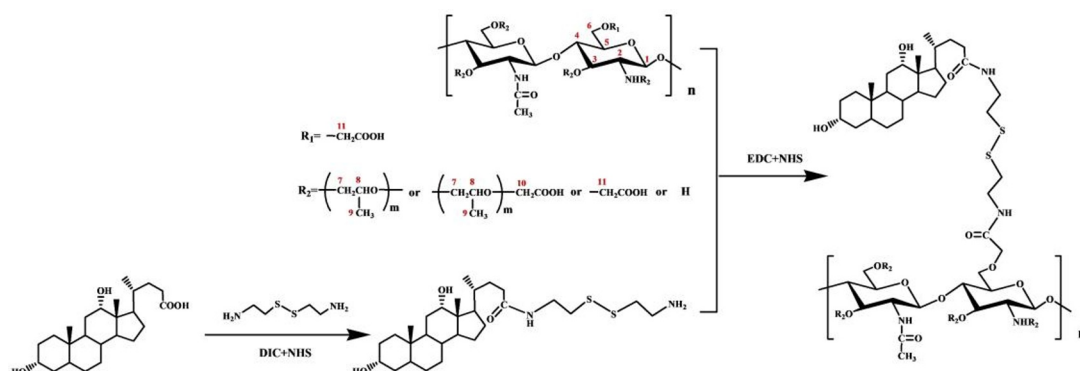


Fig. 1. Synthetic route of HPCMS-SS-DOCA.

2.2.1 Synthesis of deoxycholic acid-cystamine (DOCA-SS-NH₂)

A quantity of 1.06 g of cystamine dihydrochloride was dissolved in 3 mL of formamide, after which 340 μL of triethylamine was gradually added. The resulting mixture was stirred for 1 hour under normal temperature conditions in a sealed container to yield a cystamine solution. 0.4634 g of DOCA was added with 0.134 g of NHS and 180 μL of DIC, sealed, and 3 mL of DMF was injected into it to fully dissolve it. The mixture underwent stirring for 4 hours at room temperature, resulting in a DOCA activated ester solution. This activated solution was stored for 30 minutes at -20°C, then quickly filtered through an organic membrane while maintained in an ice bath to remove impurities from the DOCA activation process. Subsequently, the filtrate of the DOCA activated ester was slowly added dropwise to the cystamine solution using a syringe under ice bath conditions, and the entire mixture was stirred for 5 hours at room temperature. Post-reaction, the solution was carefully added into 50 mL of an aqueous solution with a pH of 9.0 under ice bath conditions to induce precipitation. The resulting mixture was then centrifuged at 9900 rpm for 20 minutes at 4°C, and the supernatant was discarded to isolate the DOCA-SS-NH₂ precipitate.

2.2.2 Synthesis of carboxymethyl hydroxypropyl chitosan-cystamine-deoxycholic acid (HPCMS-SS-DOCA)

0.5 g of HPCMS was dissolved in 20 mL of water, 120 mL of formamide was added gradually, and thoroughly mixed. Subsequently, 0.3048 g of NHS and 0.493 g of EDC were introduced, and the blend was stirred for 4 hours under sealed room temperature conditions to produce an HPCMS activated ester solution. The DOCA-SS-NH₂ precipitate was dissolved in 12 mL of DMSO, and slowly dripped into the HPCMS activated ester solution using a syringe. The amalgamation was sealed and agitated for 24 hours under room temperature conditions. Following the reaction, the reaction solution was shifted to a dialysis bag (M_w 3500 Da), and dialyzed with a 60% ethanol solution until it turned transparent, then relocated to ultrapure water for additional dialysis, and finally freeze-dried to procure the HPCMS-SS-DOCA polymer.

2.2.3 Preparation of blank/drug-loaded micelles

40 mg of HPCMS-SS-DOCA polymer were included in 40 mL of PBS (pH 7.4, 0.01 mol/L), thoroughly mixed, and sonicated in an ice bath for 30 minutes to enhance dissolution. The mixture was transferred into a dialysis pouch (M_w 3500 Da) and dialyzed with water for 24 hours, then filtered using a 0.45 μ m water membrane, and freeze-dried to produce HPCMS-SS-DOCA blank micelles.

Take 15 mg doxorubicin hydrochloride, add 14.7 mL DMF, add 0.3 mL triethylamine, stir in the dark for 13 h to remove the hydrochloride salt, add 20 mL formamide to 40 mg HPCMS-SS-DOCA polymer, fully mix, in the dark condition, add 10 ml alkalized doxorubicin dropwise to the polymer solution, stir for 4 h, slowly add 20 ml water to it, Mix the solution while protected from light for 24 h. Transfer the mixture into a dialysis bag (M_w 3500 Da) and perform dialysis against water in darkness for an additional 24 h. After dialysis is completed, filter with a 0.45 μ m water membrane, freeze-dry, and the HPCMS-SS-DOCA drug-loaded micelles are obtained.

2.3 Characterizations

The infrared spectra were obtained using the IS10 model Fourier transform infrared spectrometer. At room temperature and under dry conditions, 64 scans were conducted with KBr particles, with a resolution of 4 cm^{-1} and a scan range of 400~4000 cm^{-1} . NMR spectra were obtained with the JNM-ECP 600 model nuclear magnetic resonance spectrometer operating at 600.20211 MHz. The acquisition time (AQ) was set at 5.52 μ s, the relaxation time (D1) at 5.0 s, and the pulse angle at 45°. 32 scans were carried out, with TMS serving as the reference for relative displacement corresponding to the NMR spectra. The size of the micelles and their Zeta potential were measured and analyzed using the Nano-ZS90 model nanoparticle size and Zeta potential analyzer (DLS) at a test temperature of 25°C. Each sample was tested in triplicate. The morphology of both blank and drug-loaded micelles was observed using the JEM-1200EX model transmission electron microscope (TEM).

2.4 Loading capacity and encapsulation efficiency

To avoid any potential plagiarism issues and enhance the original text's clarity while adhering to the original meaning and instructions, you can rephrase it as follows: Dissolve 2 mg of doxorubicin hydrochloride in a mixed solvent where the volume ratio of formamide to water is 1:1. This will create a doxorubicin hydrochloride solution with a concentration of 100 μ g/mL. Subsequently, dilute the solution to achieve various mass concentrations. Measure the absorbance at 480 nm wavelength. Plot a standard curve for doxorubicin by using the concentration of doxorubicin as the x-axis (abscissa) and the absorbance values as the y-axis (ordinate). Please check your final text for any other potential issues before submitting.

Take 0.5 mg of the prepared drug-loaded micelles, dissolve and volumetrically dilute it to 10 mL with the mixed solvent of V(formamide):V(water)=1:1, and ultrasonicate for 30 minutes under the condition of ice bath to destroy the nano micelles and promote the release of the drug. Next, measure the absorbance at 480 nm. Using the doxorubicin standard curve, determine the mass of doxorubicin present in the drug-loaded micelles, then proceed to compute the loading capacity (LC%) and encapsulation efficiency (EE%) utilizing Equations (1) and (2).

$$LC\% = \left(\frac{W_1}{W_2}\right) \times 100\% \quad (1)$$

$$EE\% = \left(\frac{W_1}{W_3}\right) \times 100\% \quad (2)$$

In the formula: W_1 , W_2 , and W_3 respectively represent the mass of the encapsulated drug in the drug-loaded micelles, the mass of the drug-loaded micelles, and the mass of the drug added.

2.5 Experimental of in vitro drug release of drug-loaded micelles

Prepare a solution of drug-loaded micelles by dissolving 7 mg in pH 7.4 PBS to achieve a concentration of 1 mg/mL. Transfer 3 mL of the drug-loaded micelle solution into individual 3500 Da dialysis bags, and immerse them in 60 mL of pH 7.4 PBS containing GSH concentrations of 0 mM and 10 mM, respectively. The drug was released in a water bath shaker at 37 °C and 120 r/min for 48 hours, and 2 mL of dialysate was taken every period of time, three parallel samples were taken, and the corresponding dialysis medium of equal volume was promptly supplemented. The absorbance value at 480 nm wavelength was measured, the concentration of mass was determined based on the standard curve, and the total amount of drug released ($E_r\%$) was calculated using Equation (3), followed by plotting the drug release curve accordingly.

$$E_r\% = \left(\frac{V_1 C_n + V_2 (C_1 + C_2 + \dots + C_{n-1})}{m_{DOX}}\right) \times 100 \quad (3)$$

In the formula, $C_1 \sim C_n$ represent the DOX mass concentration in samples 1 to n, μ g/mL; V_1 is the initial volume of the release medium at 60 mL; V_2 is the volume of each individual sample at 2 mL; m_{DOX} is the total mass of drug in the micelles loaded with the drug, measured in μ g.

3 Results and discussion

3.1 Characterization of the structure of HPCMS, DOCA-SS-NH₂, and HPCMS-SS-DOCA

The infrared spectra for HPCMS, DOCA-SS-NH₂, and HPCMS-SS-DOCA are presented in Fig. 2. In the case of HPCMS, the peaks observed at 2973 cm^{-1} and 1457 cm^{-1} correspond to the asymmetric stretching and bending vibrations of C-H in the hydroxypropyl methyl group,

respectively. Additionally, the peaks at 1582 cm^{-1} and 1383 cm^{-1} signify the asymmetric and symmetric stretching vibrations of the carboxylate group ($-\text{COO}^-$), respectively. For DOCA-SS- NH_2 , the stretching vibration peaks at 2934 cm^{-1} and 2862 cm^{-1} pertain to C-H bonds in $-\text{CH}_3$ and $-\text{CH}_2-$ groups. Further, bending vibration peaks for C-H in these groups appear at 1447 cm^{-1} and 1380 cm^{-1} . Notably, the amide I and II bands are discernible at 1660 cm^{-1} and 1545 cm^{-1} , revealing the conversion of the carboxyl group in DOCA to an amide bond. Upon comparison with the HPCMS spectrum, the spectrum of HPCMS-SS-DOCA reveals an increase in the absorption peak intensities at 2934 cm^{-1} and 2862 cm^{-1} . It also shows the disappearance of the asymmetric stretching vibration peak of carboxymethyl at 1582 cm^{-1} and the symmetric peak at 1383 cm^{-1} . The presence of bending vibration peaks for C-H in $-\text{CH}_3$ and $-\text{CH}_2-$ from DOCA-SS- NH_2 , along with the amide I and II bands, underscore the successful synthesis of HPCMS-SS-DOCA.

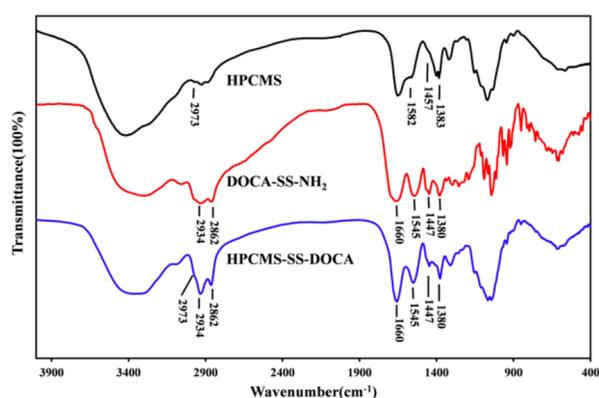


Fig. 2. Infrared spectra of HPCMS, DOCA-SS- NH_2 , and HPCMS-SS-DOCA.

Fig. 3 displays the nuclear magnetic resonance hydrogen spectra of HPCMS, DOCA-SS- NH_2 , and HPCMS-SS-DOCA. In the case of HPCMS, the proton peaks of the methyl groups on the hydroxypropyl at both the C_3 and C_6 hydroxyls on the sugar ring are observed at chemical shifts δ 1.15 and 1.26 ppm. Additionally, the proton peaks of the methyl groups on the hydroxypropyl on the amino group at the C_2 position on the sugar ring are present. The proton peak of the $-\text{CH}_2-$ on the carboxymethyl substitution on the amino group at the C_2 position on the sugar ring is observed at chemical shift δ 3.42 ppm. Moreover, the proton peaks of the $-\text{CH}_2-$ on the carboxymethyl substitution on the hydroxyls at the C_3 , C_6 , and hydroxypropyl on the sugar ring are seen at chemical shifts δ 4.23~4.32 ppm. For DOCA-SS- NH_2 , the characteristic peaks appearing between chemical shifts δ 0.59~2.31 ppm are the proton peaks of DOCA, among which the methyl proton peaks at the C_{18} , C_{19} , and C_{21} positions on the deoxycholic acid correspond to the chemical shifts δ 0.59 ppm (a), 0.85 ppm (b), and 0.92 ppm (c); the two groups of peaks appearing at 2.73~2.89 ppm and chemical shifts δ 3.30~3.38 ppm are the proton peaks of the $-\text{CH}_2-$ near S and N in cystamine; a group of peaks appearing at chemical shifts δ 7.96~8.24 ppm are the proton absorption peaks of the amide bonds in the

structure; this indicates that DOCA-SS- NH_2 is successfully synthesized. For HPCMS-SS-DOCA, compared with HPCMS, it can be seen that the methyl proton peaks substituted by hydroxypropyl on the sugar ring at chemical shifts δ 1.15 and 1.26 ppm, and the proton peaks on the sugar ring at chemical shifts δ 3.05~4.14 ppm, compared with DOCA-SS- NH_2 , it can be seen that DOCA-SS- NH_2 has the proton absorption peaks of the amide bonds at chemical shifts δ 7.96~8.24 ppm and the characteristic proton peaks of DOCA at chemical shifts δ 0.59~2.31 ppm. The above indicates that HPCMS-SS-DOCA is successfully synthesized.

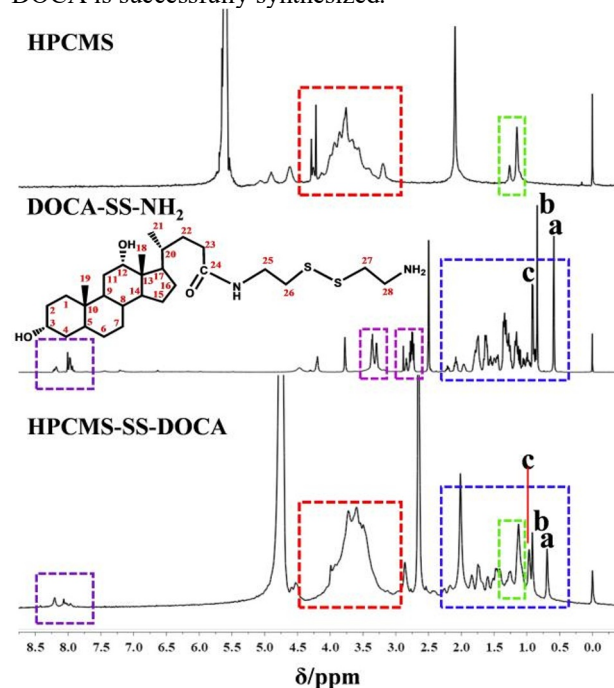


Fig. 3. NMR hydrogen spectra of HPCMS, DOCA-SS- NH_2 , and HPCMS-SS-DOCA.

3.2 Research on the micelle properties

The polymer HPCMS-SS-DOCA was successfully synthesized and used to create blank micelles and drug-loaded micelles through dialysis. Fig. 4a illustrates the particle size distribution of the micelles, while Table 1 details the average particle size, PDI, Zeta potential, drug loading, and encapsulation efficiency of the drug-loaded micelles. The prepared blank and drug-loaded micelles exhibit a single peak distribution in particle size, with PDIs of 0.303 and 0.189, respectively—indicating uniform distribution. The average particle sizes are 225.3 nm for blank micelles and 262.9 nm for drug-loaded micelles. The slightly larger size of drug-loaded micelles results from increased core volume post-DOX loading. Zeta potentials of both blank and drug-loaded micelles are negative at -6.54 and -6.57, respectively, reflecting the presence of free carboxyl groups on the HPCMS molecular chain, leading to surface charge and electrostatic repulsion between micelles for structural stability^[14].

By employing an ultraviolet-visible spectrophotometer to generate the standard curve for

DOX at 480 nm, the resulting equation for the standard curve is $y = 21.277x - 0.0102$. The absorbance value y exhibits an excellent linear correlation with the concentration x ($R^2 = 1$). The micelles' drug loading capacity is measured at 13.23%, with an encapsulation efficiency of 66.14%, demonstrating the micelles' effective drug-loading capability.

Fig. 4b depicts the observation of blank micelles and drug-loaded micelles using transmission electron microscopy. The spherical shape and good dispersibility characteristics are evident in the electron microscopy images of both types of micelles. Following the loading of DOX, the particle size of drug-loaded micelles is noted to be larger compared to that of the blank micelles. This finding aligns with the results obtained from dynamic light scattering (DLS). However, it is important to highlight that the particle size measurements obtained through TEM are significantly lower, possibly attributed to structural collapse induced by sample drying.

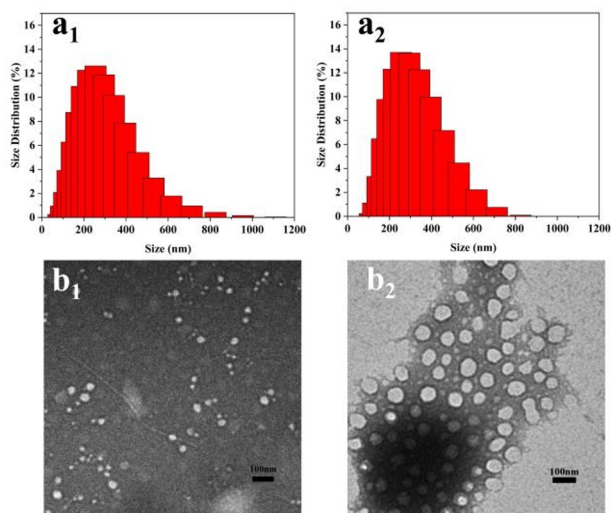


Fig. 4. Particle size distribution (a) and TEM images (b) of HPCMS-SS-DOCA and HPCMS-SS-DOCA / DOX.

Table 1. Performance characterization of HPCMS-SS-DOCA and HPCMS-SS-DOCA/DOX.

Sample	DL (%)	EE (%)	Diameter (nm)	PDI	Zeta potential (mV)
HPCMS-SS-DOCA	/	/	225.3±1.4 4	0.303±0 .031	-6.54±0.82
HPCMS-SS-DOCA/DOX	13.23	66.14	262.9±2.0 5	0.189±0 .029	-6.57±1.13

3.3 Study on the in vitro drug release performance of HPCMS-SS-DOCA drug-loaded micelles

Fig. 5 displays the drug release profile, illustrating two distinct stages of drug release from the drug-loaded micelles. Initially, there is a burst release phase where the drug concentration in the medium rises rapidly over the first ten hours. This is attributed to the rapid detachment of the drug adsorbed on the micelle surface upon contact

with the medium. Subsequently, a stable release phase ensues. Interestingly, the drug-loaded micelles in the GSH-free release medium exhibit minimal additional drug release. In contrast, the presence of GSH in the release medium facilitates the reduction of disulfide bonds in the polymer structure. This leads to the disruption of the polymer structure and deformation of the core-shell configuration of the micelles, resulting in a gradual release of encapsulated DOX. Notably, within 48 hours, the drug release percentage from the micelles in the GSH-containing medium is 52.67%, while the release percentage from the micelles in the GSH-free medium is 25.57%. The results show that it has good protection ability for DOX in normal tissues and can deliver the drug smoothly to the tumor tissue. After reaching the tumor tissue, the drug-loaded micelles have obvious redox responsiveness, which enables the drug to be released in large quantities in the local tumor tissue, playing the role of targeted treatment. This micelle has great application potential in tumor treatment.

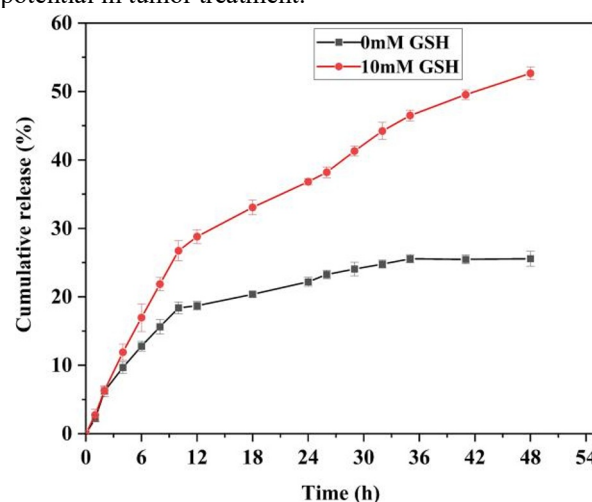


Fig. 5. Kinetics curve of drug release from the drug-loaded micelles.

4 Conclusion

By conducting an amidation reaction, an amphiphilic polymer (HPCMS-SS-DOCA) with redox responsiveness was successfully synthesized. Carboxymethyl hydroxypropyl chitosan (HPCMS) was utilized as the hydrophilic group, while cystamine-modified deoxycholic acid (DOCA-SS-NH₂) served as the hydrophobic group. Subsequently, the polymer underwent self-assembly through dialysis to produce drug-loaded micelles. Within these micelles, DOCA-SS-NH₂ acted as the hydrophobic core and HPCMS functioned as the hydrophilic shell. Analysis using transmission electron microscopy (TEM) revealed that the drug-loaded micelles exhibited a spherical shape and excellent dispersion characteristics. Dynamic light scattering (DLS) measurements demonstrated an average particle size of 262.9 nm, a polydispersity index (PDI) of 0.189, and a Zeta potential of -6.57 for the micelles. These results confirmed the micelles' small size, uniform distribution, and stability. Furthermore, the drug loading

and encapsulation efficiency were determined to be 13.23% and 66.14%, respectively, indicating the micelles' proficient encapsulation of hydrophobic drugs. In vitro drug release studies showed that, in a reductive environment, the drug release amount from the micelles within 48 hours reached 52.67%, while in a non-reductive environment, the release amount was only 25.57%. This finding underscored the micelles' effective response to redox stimuli.

In this paper, an amphiphilic polymer was synthesized using carboxymethyl hydroxypropyl chitosan as the raw material, which broadens the application scope of chitosan in the drug delivery system and provides a new idea for the synthesis and modification of chitosan. The drug-loaded micelles prepared by the amphiphilic polymer have good encapsulation ability for hydrophobic drugs and better drug release performance in a reductive environment, indicating that this polymer micelle has good delivery ability for antitumor hydrophobic drugs and can achieve the purpose of targeted treatment, increasing the local concentration of drugs in tumor tissues and reducing drug toxicity. It has laid a solid foundation for subsequent in vivo experiments.

References

1. Jindal A, Thadi A, Shailubhai K. (2019) Hepatocellular carcinoma: Etiology and current and future drugs[J]. *Journal of Clinical and Experimental Hepatology*, 9(2): 221-232. <https://doi.org/10.1016/j.jceh.2019.01.004>
2. Torchilin V P. (2001) Structure and design of polymeric surfactant-based drug delivery systems [J]. *Journal of controlled release*, 73(2-3): 137-172. [https://doi.org/10.1016/S0168-3659\(01\)00299-1](https://doi.org/10.1016/S0168-3659(01)00299-1)
3. Zhao N, Wu B Y, Hu X L, Xing D. (2017) NIR-triggered high-efficient photodynamic and chemocascade therapy using caspase-3 responsive functionalized upconversion nanoparticles[J]. *Biomaterials*, 141: 40-49. <https://doi.org/10.1016/j.biomaterials.2017.06.031>
4. Chuang C Y, Don T M, Chiu W Y. (2009) Synthesis of chitosan-based thermos-and Ph-responsive porous nanoparticles by temperature-dependent self-assembly method and their application in drug release [J]. *Journal of Polymer Science Part A: Polymer Chemistry*, 47(19): 5126-5136. <https://doi.org/10.1002/pola.23564>
5. Xie P, Liu P. (2020) pH-responsive surface charge reversal carboxymethyl chitosan-based drug delivery system for pH and reduction dual-responsive triggered DOX release [J]. *Carbohydrate Polymers*, 236: 116093. <https://doi.org/10.1016/j.carbpol.2020.116093>
6. Wang Y, Han N, Zhao Q, Bai L, Li J, Jiang T, Wang S. (2015) Redox-responsive mesoporous silica as carriers for controlled drug delivery: A comparative study based on silica and PEG gatekeepers [J]. *European Journal of Pharmaceutical Sciences*, 72: 12-20. <https://doi.org/10.1016/j.ejps.2015.02.008>
7. Wang K, Liu N, Zhang P, et al. (2016) Synthetic Methods of Disulfide Bonds Applied in Drug Delivery Systems [J]. *Current Organic Chemistry*, 20(14): 1477-1489. <https://doi.org/10.2174/1385272820666151207194002>
8. Santos V P, Marques N S S, Maia P, et al. (2020) Seafood Waste as Attractive Source of Chitin and Chitosan Production and Their Applications [J]. *International Journal of Molecular Sciences*, 21(12): 4290. <https://doi.org/10.3390/ijms21124290>
9. Majidi H J, Babaei A, Kazemi-pasarvi S, et al. (2021) Tuning polylactic acid scaffolds for tissue engineering purposes by incorporating graphene oxide-chitosan nano-hybrids [J]. *Polymers for Advanced Technologies*, 32(4): 1654-1666. <https://doi.org/10.1002/pat.5202>
10. Madni A, Kousar R, Naeem N, et al. (2021) Recent advancements in applications of chitosan-based biomaterials for skin tissue engineering [J]. *Journal of Bioresources and Bioproducts*, 6(1): 11-25. <https://doi.org/10.1016/j.jobab.2021.01.002>
11. Li J, Zhuang S. (2020) Antibacterial activity of chitosan and its derivatives and their interaction mechanism with bacteria: Current state and perspectives [J]. *European Polymer Journal*, 138: 109984. <https://doi.org/10.1016/j.eurpolymj.2020.109984>
12. Fan M, Hu Q, Shen K. (2009) Preparation and structure of chitosan soluble in wide pH range [J]. *Carbohydrate Polymers*, 78(1): 66-71. <https://doi.org/10.1016/j.carbpol.2009.03.031>
13. Sun J X, Wang T B, Chen X Y, et al. (2022) Preparation of poly mannuronic acid micelle and durg-loading ability [J]. *Journal of Qingdao University of Science and Technology (Natural Science Edition)*, 43(1): 21-27. <https://doi.org/10.16351/j.1672-6987.2022.01.003>
14. Zhu A, Yuan L, Lu Y. (2007) Synthesis and aggregation behavior of N-succinyl-o-carboxymethylchitosan in aqueous solutions [J]. *Colloid and Polymer Science*, 285: 1535-41. <https://doi.org/10.1007/s00396-007-1716-7>